S. Michael Angel* and Nathaniel R. Gomer
Department of Chemistry and Biochemistry,
The University of South Carolina,
Columbia, South Carolina 29208

Shiv K. Sharma
Hawaii Institute of Geophysics & Planetology,
University of Hawaii,
1680 East-West Rd, POST #602,
Honolulu, Hawaii 96822

Chris McKay
NASA Ames,
Building 245 Room 212, M.S. 245-3,
Moffett Field, California 94035

Remote Raman Spectroscopy for Planetary Exploration: A Review

In this review, we discuss the current state of standoff Raman spectroscopy as it applies to remote planetary applications, including standoff instrumentation, the technique's ability to identify biologically and geologically important analytes, and the feasibility to make standoff Raman measurements under various planetary conditions. This is not intended to be an exhaustive review of standoff Raman and many excellent papers are not mentioned. Rather it is intended to give the reader a quick review of the types of standoff Raman systems that are being developed and that might be suitable for astrospectroscopy, a look at specific analytes that are of interest for planetary applications, planetary measurement opportunities and challenges that need to be solved, and a brief discussion of the feasibility of making surface and plume planetary Raman measurements from an orbiting spacecraft.

Received 11 November 2011; accepted 14 November 2011.
* Author to whom correspondence should be sent. E-mail: angel@chem.sc.edu.
DOI: 10.1366/11-06535

Index Headings: **Planetary Raman; Standoff Raman; Astrospectroscopy; Laser-induced breakdown spectroscopy; LIBS; Laser-induced fluorescence; LIF; Europa; Enceladus; Astrobiology.**

INTRODUCTION

Raman spectroscopy has been proposed for astrospectroscopy as a potential mineralogical

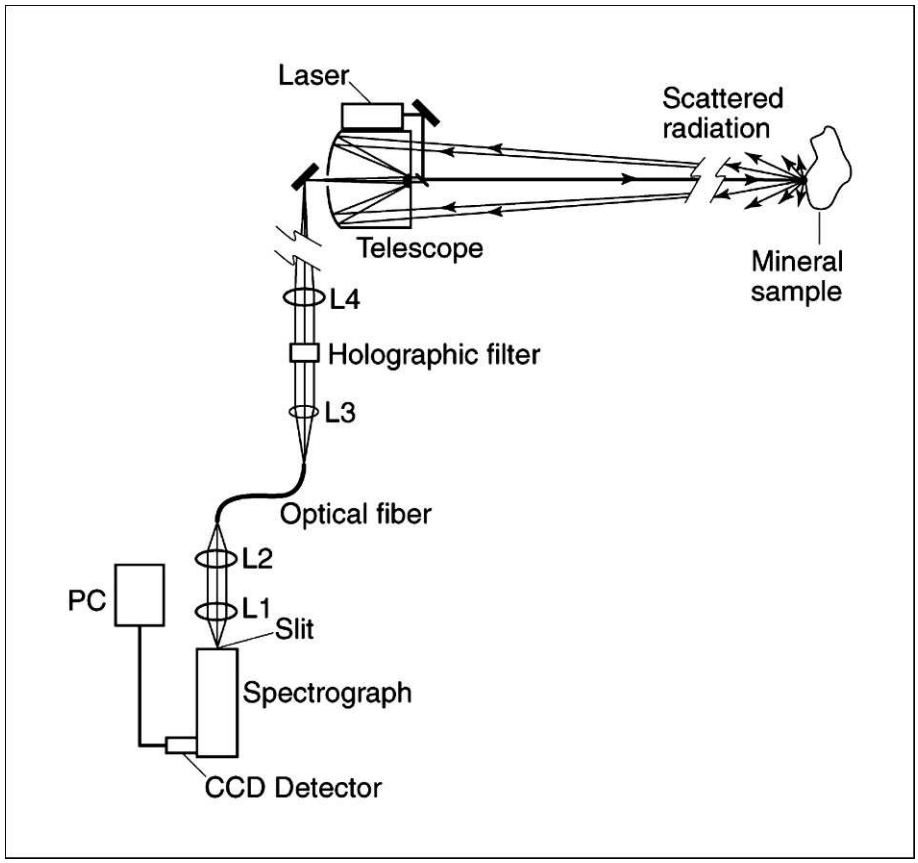

FIG. 1. Schematic diagram of a fiber-coupled standoff Raman measurement system (Reproduced with permission from Ref. 9).

analysis system to explore the Moon,[1] Mars,[2,3] and Venus[4,5] from planetary landers and rovers. Raman has several distinct advantages over other spectroscopic techniques that have been used on past missions. For planetary applications, the sharpness of Raman spectral features of minerals allows for much less ambiguous detection, especially in the presence of mixtures. Visible, near-infrared, thermal, reflection, and emission spectroscopy of minerals and compounds all suffer from broad overlapping spectral features,[2] which complicate interpretation of their spectra from which more than one mineralogical solution can be typically derived. For minerals, organic and biogenic mineral analysis, Raman spectroscopy can provide ground truthing in a global satellite remote sensor, using visible-infrared imaging from orbit for pre-selection of rock samples prior to caching for potential sample return missions. Small portable remote Raman systems, which are suitable for planetary rovers and landers, have been shown to be effective in identifying hydrous and anhydrous minerals and ices. Many remote Raman systems have been tested to distances greater than 120 m.[6–9]

Raman spectroscopy is based on inelastic scattering of light, and was discovered experimentally in 1928 by C. V. Raman.[10] The Raman technique yields information about vibrational and rotational energy levels of molecules as frequency shifts from the frequency of the exciting light source [$\Delta cm^{-1} = (\nu_0 \pm \nu_i) - \nu_0$], where ν_0 is the absolute frequency of incident light in cm^{-1} and ν_i are vibrational frequencies of the molecule. In modern Raman spectroscopy, samples are normally illuminated by a laser at a much higher frequency than that of the vibrational or rotational frequencies of interest. The elastically scattered light is rejected using a combination of extremely narrow band notch filters and proper design of the receiving spectrographs. The remaining (inelastically scattered) light shows diagnostic emission peaks that occur at wavelengths shifted from the exciting laser line by amounts equal to the energy of the excited or relaxed vibrational or rotational states. Thus, using strictly visible light sources and receivers Raman spectroscopy can yield complementary information about the vibrational transitions observed in infrared emission or reflection spectra. Raman spectroscopy is not directly equivalent to infrared (IR) spectroscopy, as the strengths of individual features can be quite different between IR and Raman spectroscopy due to different selection rules. The activity of Raman vibrational modes is a function of the change in polarizability during the vibrational mode *i*, whereas the activity of infrared modes is associated with the change in permanent dipole moment during a normal mode of molecular vibration. Raman spectra of samples contain a wealth of information that can be used to identify minerals and chemical compounds based on the vibrational frequencies, relative intensities, and number of bands in the spectra.[1,11–15] It can also be used to characterize crystalline polymorphs[16,17] and amorphous versus crystalline ices and clathrates.[18–22]

Raman spectroscopy is typically envisioned as an in situ analysis technique as it requires a strong monochromatic exciting source and highly efficient spectral measurement apparatus. However, the potential for performing Raman analysis remotely was first proposed as early as 1965,[23] and it was explored theoretically and experimentally as early as 1970 by Hirschfeld for long-range atmospheric measurements.[24–26] Small systems for moderate range standoff Raman measurements were first described in the 1990s.[27] Carter et al. have reported standoff detection of high explosive materials at 50 meters in ambient light conditions using a small Raman instrument.[28] Sharma et al. measured remote Raman spectra of minerals and organic compounds to 100 m.[3,29] Chen et al. reported detection of Raman spectra of organic liquids with a single 532 nm

laser pulse at a distance of 213 m.[30] Using semi-portable equipment, Wu et al. have reported on Raman spectroscopic identification of man-made organic compounds at distances of over half a kilometer.[31]

A remote Raman system with Raman imaging capability has potential for determining mineral distribution and composition on a rock surface by comparing a set of Raman images collected for various minerals. Carter et al. have developed a fiber-optic and directly coupled telescopic remote Raman imaging system based on an acousto-optical tunable filter (AOTF) at a distance of 10 m.[32] Both continuous wave (CW) and pulsed laser excitation were used for evaluating the AOTF-based remote Raman imaging system performance. Prospects of using remote Raman imaging and spectroscopy of minerals on planetary surfaces from an orbiting platform have also been discussed.[33]

INSTRUMENTATION

Standoff System Setup and Parameters. The components of a standoff Raman system are similar to those of a conventional Raman system, comprising a laser, collection optics, spectrometer, detector, and optical filters. The main distinction for standoff systems is the incorporation of a telescope for collection of scattered radiation, allowing analysis of a target meters away from the system.[34] Continuous wave and pulsed lasers have both been implemented, with pulsed lasers the preferred choice for their ability to be coupled with gated detectors for measurements under ambient light conditions. A charge-coupled device (CCD) or intensified CCD (ICCD) array is the most common detector, with ICCDs used extensively with pulsed lasers. Sharma et al. stated that small f-number spectrometers perform better than larger f-number spectrometers for standoff systems.[9] Figure 1 shows a typical fiber-coupled standoff Raman system.

System Geometries. The geometry of the laser and telescope with regard to the location of the sample is typically setup in one of two ways: either a co-axial or an oblique geometry (Fig. 2). The co-axial geometry places the laser beam on the optical axis of the telescope by using a prism or dielectric mirrors. This geometry is beneficial in that it does not require realignment when the sample distance changes.[34] The drawback to this geometry is a loss of laser power due to the transmission optics, specifically through the prisms.[34] The oblique geometry places the laser next to the telescope but ensures that the laser and sample are focused onto the same target. This geometry is beneficial in that it retains the full power of the laser. The drawback is the need to realign the system if the target or sample distance changes.[9] Sharma showed that co-axial systems offer a wider range of sampling depths, while oblique systems offer higher signal intensities.[9]

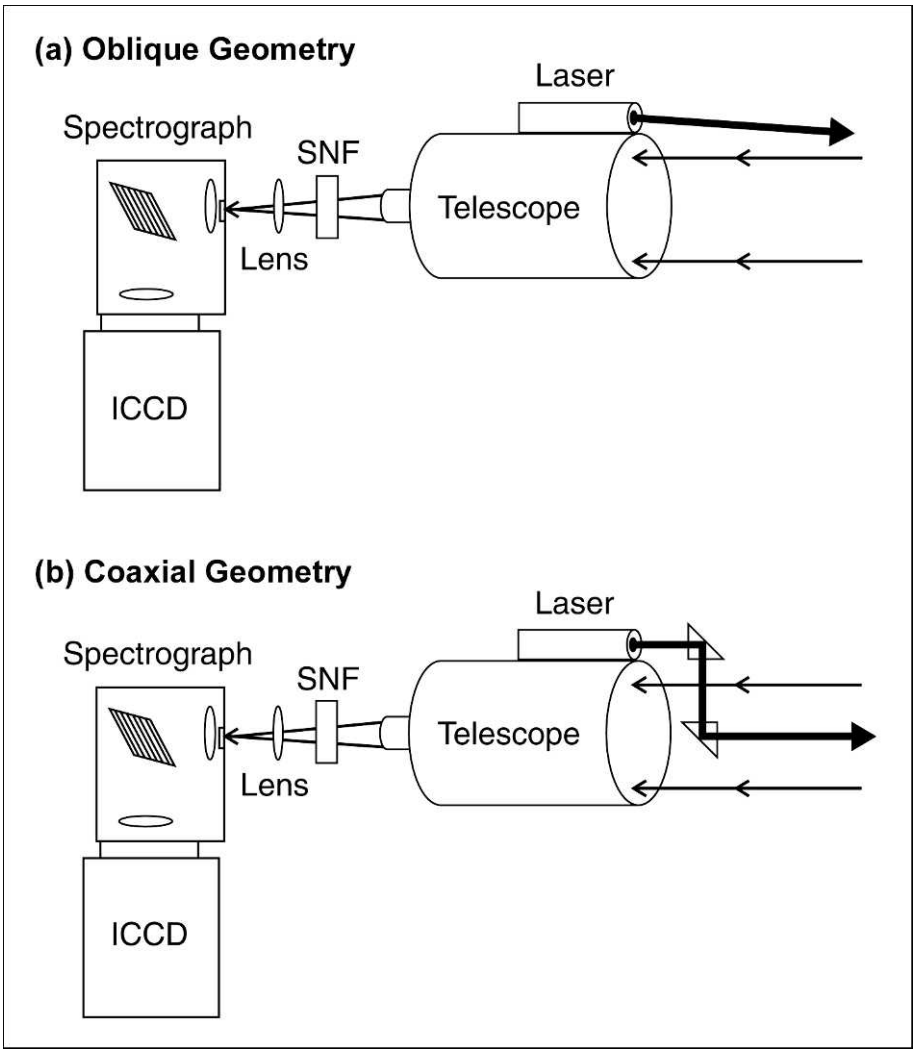

FIG. 2. Diagrams of (a) oblique and (b) coaxial directly coupled standoff Raman system geometries. SNF: Laser blocking filter.

System Coupling. Standoff Raman systems can couple the output of the telescope to the spectrometer in two different ways: directly using lenses or with the use of an optical fiber. Misra et al. showed that a directly coupled system offers better system performance over a fiber-coupled system by a factor of 10 for a system with coaxial geometry.[8] An oblique geometry system also displayed an improvement, but only by a factor of 1.6. Sharma also stated that standoff fiber-coupled systems allowed a sampling depth of ± 20 cm around the focal point, while directly coupled systems allowed a sampling depth of

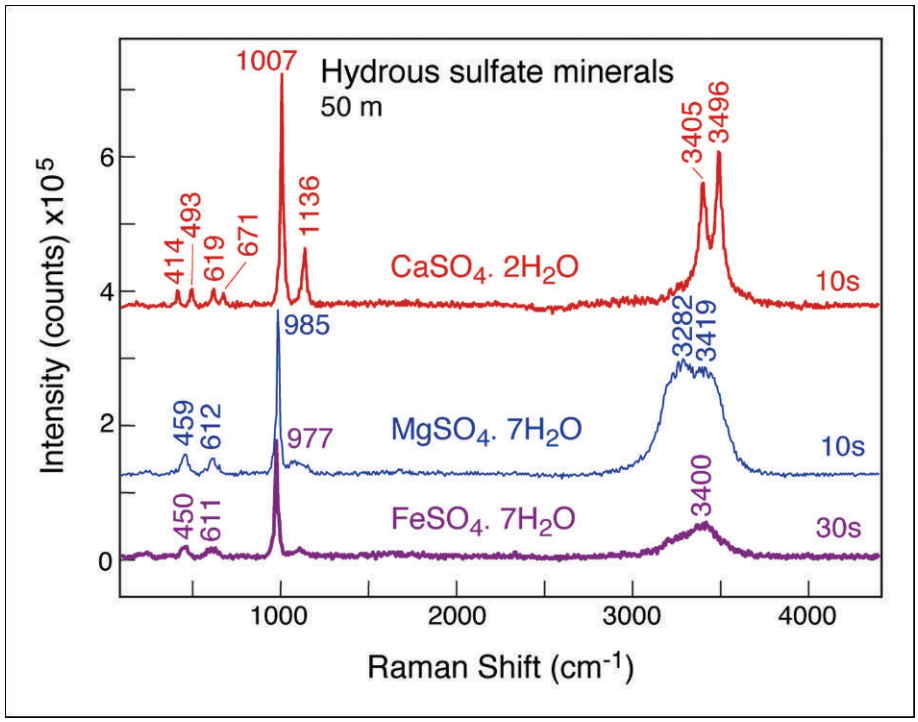

Fig. 3. Standoff Raman spectra of various hydrous sulfate minerals from a distance of 50 meters. Sulfate stretching bands are evident around 1000 cm^{-1}, while O–H stretching bands are observed between 3000 and 3500 cm^{-1} (Reproduced with permission from Ref. 74).

±15 m. Both configurations have proven useful for planetary applications because of their small size and mass and low power requirements.[9]

Time-Resolved Measurement Parameters. Utilizing a pulsed laser with a gated ICCD detector offers the potential to make time-resolved measurements in addition to ambient measurements.[28] This approach can allow avoidance of fluorescence in luminescent minerals[35] or the creation of a combined Raman/laser-induced fluorescence (LIF) instrument that is capable of greater accuracy in the identification of an unknown sample.[3] Sharma has reported that a typical gate delay of 10 ns is needed to collect Raman without fluorescent interference in a Raman/LIF system.[9] Time-resolved fluorescence data has been able to identify biogenic materials from organic and inorganic compounds.[9]

Previous Significant Standoff Results. One of the first standoff Raman systems was implemented by Angel et al., where a portable CW laser system was used to measure various organic and inorganic waste compounds at distances up to 16.7 meters, using excitation wavelengths of 488 nm and 809 nm.[27] In 2002, Sharma et al. used a portable pulsed laser at 532 nm to measure geological samples, including silicates and carbonates, at distances up to 66 meters.[6] Since then, geological samples have been measured at a distance up to 120 meters.[22] Up until this point, all standoff measurements were conducted in dark conditions, typically at night, to avoid ambient light.

In 2005, Carter et al. reported that Raman spectra could be collected in ambient light conditions by using a gated ICCD detector in place of the standard CCD and utilizing a pulsed laser, which allowed for the detection of explosives from 15 meters away.[28] The combination of using a pulsed laser with a gated detector changed how standoff Raman could be conducted outside of the laboratory. This includes making Raman measurements using only a single laser pulse[36] and making time-resolved measurements,[35] which will be discussed in greater detail later. It also allowed the avoidance of luminescence, which is difficult to do using visible excitation wavelengths.

Many improvements in standoff Raman instrumentation have been for the purposes of measuring high explosives. These same systems, however, can be suitable with modification to planetary applications. Since 2005, standoff Raman has been implemented in new ways and implemented in different environments. Gaft et al. developed a standoff Raman system in the ultraviolet (UV) region, measuring explosives from 30 meters.[37] They reported that using 266 nm excitation gave higher Raman scattering intensity by a factor between 100 and 200 over 532 nm excitation. Wu et al. developed a standoff UV Raman LIDAR system that was adapted to fit in a motor-van in order to have a mobile Raman system that could detect chemical spills up to 500 meters away.[31] In 2009, a visible standoff system was utilized in a variety of environmental conditions, including rain and snow, and was able to detect and unambiguously identify explosives from 50 meters, without experiencing any environmental interference, most notably by water.[38] Porter et al. developed a scanning standoff Raman system for Raman imaging of chemicals at a distance of ~100 m with 2 mm resolution.[39]

Standoff systems developed for planetary measurements have also improved. The focus has been on conducting standoff measurements on important planetary analytes[40] and making measurements under conditions comparable to what will be found on other planets.[9,41,42] These advances will be discussed in greater detail later in the paper.

TARGETS

A key goal for astrobiology is the search for evidence of life on the other worlds of our solar system. The first step in this search is the characterization of the geological and hydrological settings. This is often described as the search for liquid water. However, while water is the essential medium for life, organic material is what composes life. Thus, as the search moves beyond the search for habitable environments and toward the search for evidence of life itself, the detection and characterization of organics is required.

There are many applications for active spectroscopy dealing with organic analysis on planetary missions. We discuss three examples that illustrate the range of opportunities and might be considered *Grand Challenge*s. These are the search for organics on Mars, the search for a landing site on the surface of Europa, and the characterization of complex organics in the plume of Enceladus.

Celestial Bodies. ***Mars.*** Mars is the closest planet to Earth and was once thought to have had an environment similar to Earth's, with the belief that water was present on Mars at some point; thus, the search for water is a critical component of Mars exploration. The current atmospheric conditions on Mars are much different. The Martian atmosphere contains approximately 95% CO_2. The average atmospheric pressure is between 6 and 10 mbar and daily temperatures fluctuate between 170 K and 290 K throughout the year.[43] Volcanic out-gassing is believed to have contributed to the presence of sulfur on Mars, where the sulfur cycle is believed to have played a major role in Martian history.[44] Important sulfur-bearing analytes include SO_2 and H_2S in addition to sulfates (e.g., $FeSO_4$), sulfide-bearing minerals (e.g., FeS), and hydrous sulfates (e.g., $CaSO_4{\cdot}2H_2O$).[44] Figure 3 shows the Raman spectra of various hydrous sulfates. The addition of water to anhydrous sulfate results in shifting of the symmetric stretching mode of sulfate ion to lower frequency because of hydrogen bonding between the oxygen of sulfate ions and water. It is noteworthy that the symmetric S–O stretch at 985 cm^{-1} for $MgSO_4{\cdot}7H_2O$ shifts to 977 cm^{-1} when Mg is substituted by Fe (see Fig. 3).

In 2007, Sharma et al. first conducted standoff Raman measurements under Martian conditions, utilizing a combined Raman/laser-induced breakdown spectroscopy (LIBS) system.[45] Samples analyzed were sulfur-containing minerals (e.g., gypsum), calcite, benzene, and elemental sulfur at distances up to 8.6 m. Pyrite and chalcopyrite were also tested, but Raman spectra could not be obtained from either due to their weak Raman scattering intensity. Similarly, Dreyer et al. conducted Raman/LIBS measurements under Martian conditions the same year, reporting extensive LIBS results.[42] The Raman results reported for benzene and calcite showed no peak broadening or shifting due to changes in pressure. Sharma et al. also designed a combined Raman/LIF system that was adapted for a Martian lander and was capable of making real-time measurements and could detect LIF up to 5 km distant.[3]

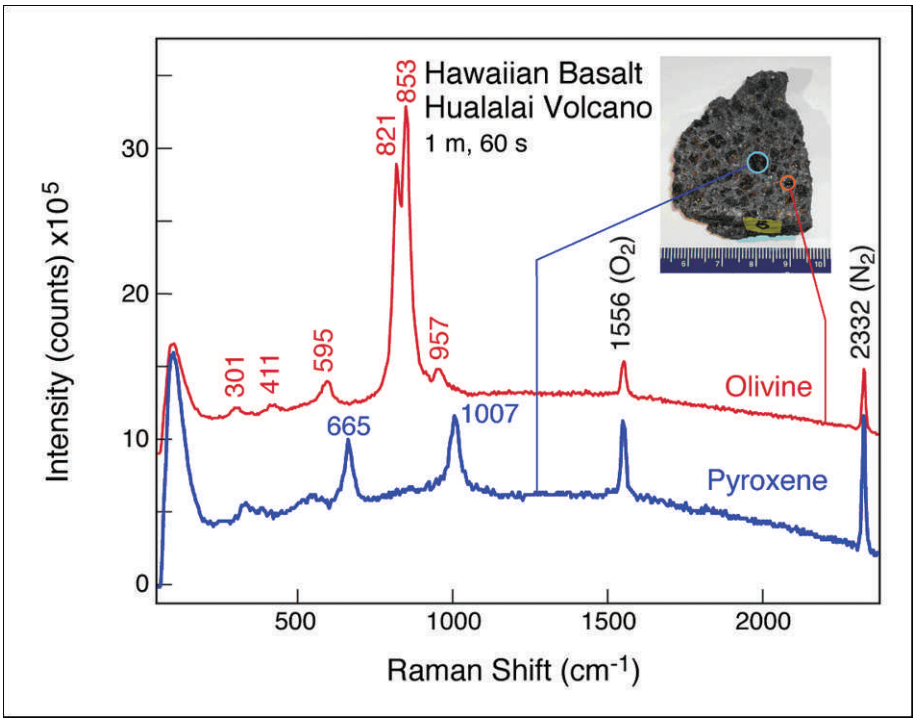

Fig. 4. Remote Raman spectra of pyroxene and olivine found within Hawaiian basalt from the Hualalai Volcano (Reproduced with permission from Ref. 74).

Portable Raman systems have also been taken into Mars-like conditions at remote Earth sites. In 2011, Rull et al. took a portable Raman system into the Arctic to make in situ measurements of glacier ice from distances up to 120 meters and were able to observe spectral differences due to the different conditions of ice formation.[46] In 2010, Edwards et al. took a portable Raman system to the Arabian desert and detected organic molecules in evaporitic minerals, such as carbonate or gypsum, that indicated the presence of extremophilic cyanobacteria.[47] In 2010, Villar et al. analyzed lava rock samples collected near a volcano in Kona, Hawaii, detecting important planetary analytes, such as chlorophyll and gypsum, in a complex matrix.[48] Finally, in 2007 Edwards et al. took a portable system to the Rio Tinto, a river rich in iron and sulfates with an acidic pH.[49] This site is widely considered an analog to the El Capitan region of the Meridiani Planum on Mars. Within the river, key biomarkers, such as carotenoids and scytonemin, and minerals, such as jarosite and gypsum, were detected.

Martian meteorites have been analyzed by Raman spectroscopy.[50] The meteorite Zagami was determined to have high amounts of pyroxene and was formed through high-temperature processes based on the forms of pyroxene found.[51] Analysis of other meteorites led to the identification of major, minor, and trace components, showing different stages of crystallization in sulfates and identifying major silicate components such as pyroxene and olivine, in order to determine composition.[52] Figure 4 shows the Raman spectra of pyroxene and olivine found within Hawaiian volcanic basalt.

The search for organics on Mars is currently being conducted using rovers such as the Mars Science Laboratory (launched in November 2011, landing

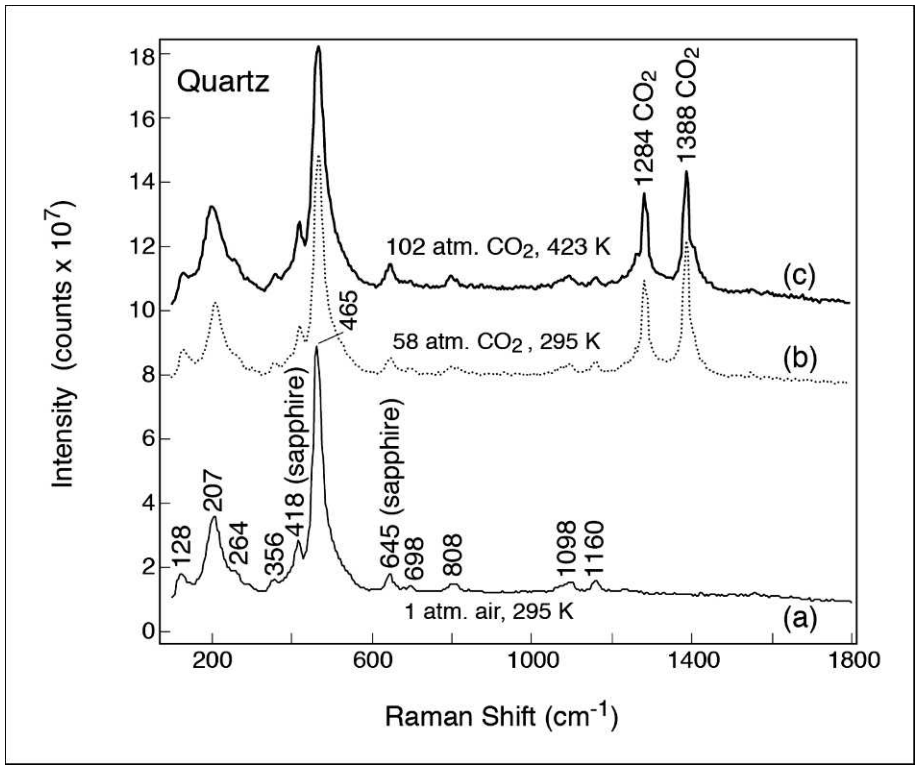

FIG. 5. Remote Raman spectra of quartz under (a) air and (b) gaseous CO_2 and (c) supercritical CO_2 (Reproduced with permission from Ref. 41).

on Mars August 2012). It will have a sophisticated system for sample analysis (Sample Analysis on Mars, or SAM)[53] that will be able to detect organic materials in several modes. However, selecting samples for analysis using SAM is a significant issue for several reasons. First, the level of organics on Mars is expected to be low and careful sample selection will probably be required. Second, the difficulty of moving the rover and manipulating the sample collection systems remotely from Earth means that only a limited number of sampling sites can be fully accessed. Finally, only a limited number of samples can be processed.

On the Mars Science Laboratory, sample selection will be guided by a LIBS instrument (the ChemCam spectrometer).[54] This instrument will provide information on elemental composition but will not be able to detect low levels of organics. Thus, there is interest in the development of a stand-off capability to detect organics at low levels (ppm and below) in soils and rocks on Mars. The goal of this detection is not a complete and detailed analysis but as a method for selection of samples for collection and more detailed analysis with instruments such as SAM. Both Raman and UV fluorescence are being considered as possible approaches to stand-off selection of samples on Mars for organic analysis.[35,45]

The Mars Microbeam Raman Spectrometer (MMRS) is a lander-based remote Raman system developed by Wang et al. with the goal of identifying major, minor, and trace amounts of organic and inorganic components of minerals.[55] The system utilizes an innovative laser probe that is mounted in a lander's robotic arm.[56] The probe head extends out to the sample of interest and makes surface Raman measurements using a point-count method developed by Haskin that allows estimations of the relative proportions of different mineral constituents.[2] The system is also capable of characterizing textural features of a rock sample as well as its chemical components. The MMRS was intended to be a part of NASA's Spirit missions and was given high priority for inclusion on the Mars Science Lab mission.

The ExoMars mission is a venture by the European Space Agency for the exploration of Mars and to study geological samples and search for evidence of life. The mission will include both an orbiter and a lander, with the orbiter scheduled to launch in 2016 and the lander in 2018. The lander will feature the first Raman spectrometer to study Mars and will be coupled with a LIBS system for mineral analysis. The system can operate in two different fashions: a micro-mode and a macro-mode. In micro-mode, the system will look at mineral samples brought into the lander and crushed into fine grains (20–100 μm in size) by a separate component of the lander. In macro-mode, a probe attached to the lander's robotic arm will be extended out to samples on the planet's surface, with the capability of measuring larger areas by using a larger beam diameter (a few hundred micrometers).

Venus. Two of the most important advantages of remote Raman spectroscopy over other techniques for a mission to Venus are rapid mineralogical analysis of both hydrous and anhydrous minerals and stand-off analysis at distances up to many meters.[5,41] Rapid mineralogical analysis and stand-off analysis are important to missions to Venus due to the harsh environment on the planet surface (pressure ~9.1 MPa or 90 atm and temperature ~735 K).[57] The major gas in the Venus atmosphere is CO_2, and under Venus atmospheric conditions CO_2 exists in the supercritical phase near the surface.

Remote Raman measurements conducted at the University of Hawaii on minerals under high temperatures up to 1003 K at 9 m, and under supercritical CO_2 (~95 atm and 423 K) at 1.5 m have successfully demonstrated the potential of the technique for Venus exploration.[5,41] Minerals important to Venus, such as anhydrous sulfates, carbonates, and silicates, were detected under both dark and ambient light conditions, while CO_2 was present in the spectra as a Fermi resonance doublet. The results showed that a remote Raman system would be useful on Venus to measure

dehydration and decarboxylation products, analyze surface mineralogy, and identify atmospheric constituents. Figure 5 shows the spectrum of quartz acquired under air and different CO_2 phases.

The Moon. Today, most investigations of the moon center on the analysis of lunar rock and soil samples. Future missions to the moon could incorporate a remote Raman system. Raman studies on lunar soils have identified pyroxene, feldspar, and olivine.[1] In addition, Raman has been able to deduce compositional distributions and mineral modes of certain minerals as well as estimate impact pressures from quartz peak positioning.[58]

Other Important Celestial Bodies. Europa, one of the large moons of Jupiter, has an icy surface and evidence for an ocean below the ice. The surface of Europa has features that appear to indicate ice floating on water. These include linear cracks, icebergs, and fractured ice rafts.[59,60] The evidence that the subsurface water is still present comes from the magnetic disturbance that Europa makes as it moves through Jupiter's magnetic field. The disturbance indicates a slightly conductive global ocean.[61] In the water of Europa's ocean, there may be life.[62]

On Europa the search for life has not yet advanced to the point where surface landers have been deployed. Here the goal for active spectroscopy would be to determine—from an orbiter—the best site on the surface for an astrobiology lander. The goal would be to detect organics on the surface presumably in association with geological features, such as the linear dark bands, that indicated that these organics may have come from the subsurface ocean. Concepts for detection of organics from orbital distances (>10 km) on Europa are based on pulses of a UV laser followed by Raman or fluorescence spectroscopy and are described in detail in a later section of this paper.

Finally, Enceladus is a small icy moon of Saturn, with a radius of only 252 km. Cassini data have revealed about a dozen or so jets of fine icy particles emerging from the south polar region of Enceladus.[63] The jets have also been shown to contain simple organic compounds, and the south-polar

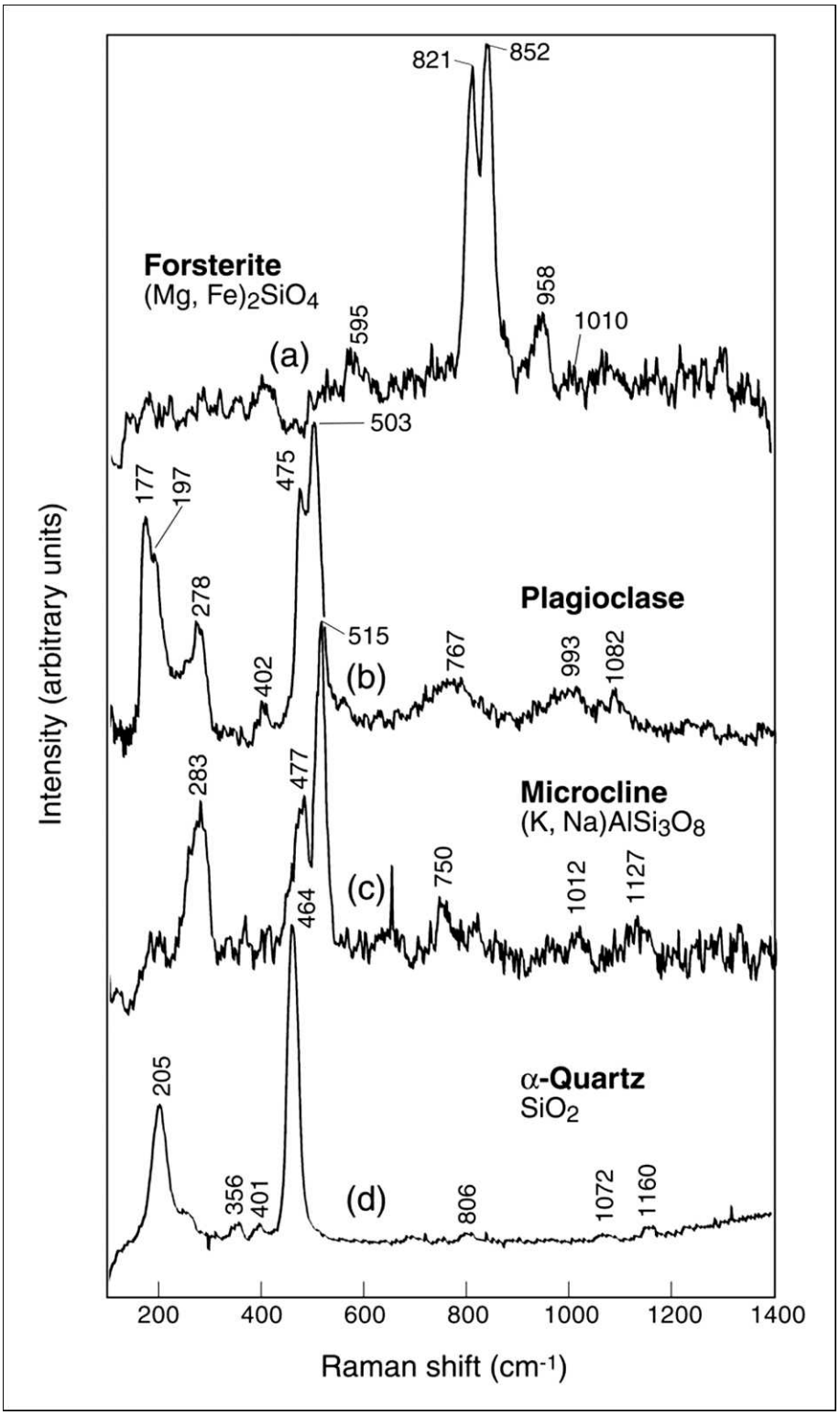

Fig. 6. Remote Raman of silicate minerals forsterite, plagioclase, microcline, and α- quartz.

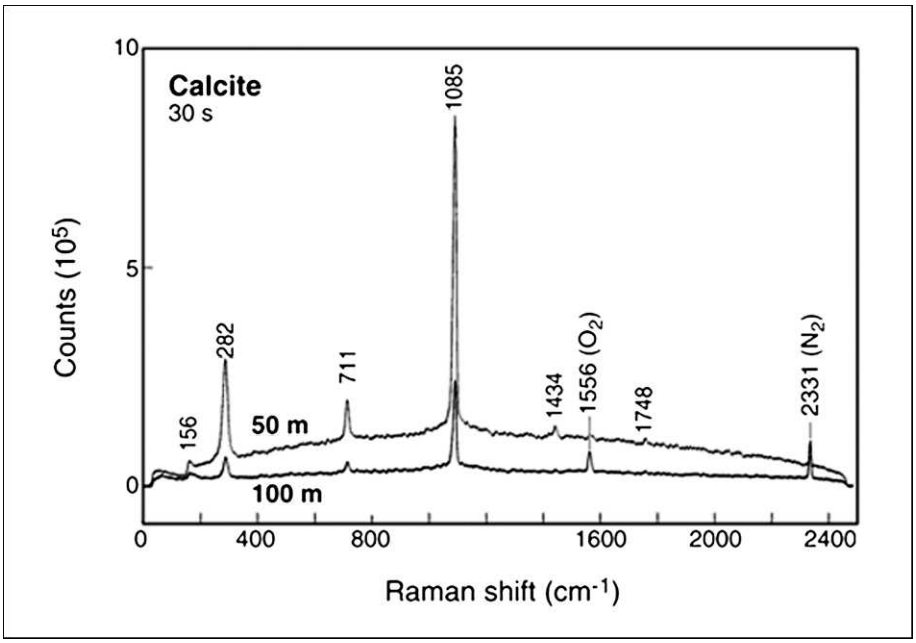

FIG. 7. Standoff Raman spectra of calcite at distances of 50 meters and 100 meters (Reproduced with permission from Ref. 9).

region is bathed in excess heat coming from below.[64,65] The possibilities for life have been discussed.[66]

The next step in the search for evidence of life on Enceladus is a search for more complex organics in the plume. A plausible target is amino acids,[67] and their distribution and chirality would be important information about the possible biogenic nature of the organics in the plume.[66] However, it is a significant challenge to safely access the plume to obtain a sample. Remote spectroscopy would provide an ability to make the necessary detection from a safe distance from the plume. Ideally the remote method would determine the presence and relative concentration of several key amino acids and their chiral properties. Jenkins et al. have reported on the characterization of amino acids using Raman spectroscopy,[68] though this technique is probably not practical in orbit since it requires long integration times and would suffer from low signal-to-noise ratio.

Analytes of Interest. Important planetary analytes can be broken into two categories: geological and biological. Geological analytes include minerals believed to be on celestial targets that can yield information about the mineral formation or history of the planet. Biological analytes of importance will indicate the presence of life or past life. In addition, they can also answer questions about the planet's history of formation.

Geological Analytes. Geological samples, such as rocks, minerals, or water, are the primary targets for planetary missions. Standoff Raman systems will look to characterize the components of a rock sample in order to learn the major, minor, and trace components it contains. The Raman spectra of minerals tend to exhibit features that are narrow, well defined, and do not overlap with other features, allowing nearly unambiguous detection.[7] Standoff Raman has proven to be a valuable tool for mineral identification with its ability to distinguish between different rock constituents at distances up to 120 meters (Fig. 6).[3,6–9,22,29,36,40,45] Raman spectroscopy has the capability to determine the temperature and pressure of formation and to differentiate between living organic material and non-living remains, such as fossils.[40] In 2005, Stopar et al. studied numerous mineral samples at a standoff distance of 10 meters and determined Raman scattering intensities for each.[40] Large, clear crystals were reported to have better scattering efficiency than darker minerals. Figure 7 shows the Raman spectrum of calcite acquired at two different standoff distances.

Many geological analytes have been proposed for Mars. The surface of Mars is rich in sulfates, specifically sulfates of magnesium, calcium, and iron.[69] Ling et al. analyzed eight different hydrous and anhydrous ferrous sulfates and determined that Raman spectroscopy was able to distinguish between all eight types, as well as establishing a greater understanding of how the ferrous sulfates could be found on Mars.[69] Similar work on a group of iron sulfates, known as copiates, was able to distinguish between different types by monitoring SO_4^{2-} peak shifts due to cationic substitutions (see Fig. 3).[70] Wang et al. were able to monitor different degrees of hydration in sulfates using Raman.[44] Raman spectroscopy was also able to distinguish between ten different types of feldspars.[71] Other important minerals include pyroxene, olivine, quartz, jarosite, and gypsum.[49,72,73]

Ice is another very important geological sample that could hold key biomarkers and is unique in that water can exist as a solid, liquid, or gas in the atmosphere. Raman has been able to distinguish between different forms of ice with conventional Raman spectrometers[18] and in remote systems (Fig. 8).[74] Ice forms II, III, and V exhibit a higher O–H bond frequency than the Ih and Ic forms, and thus can be distinguished spectroscopically.[18] Remote Raman systems have been able to distinguish phases of ice by making in situ measurements in the Arctic.[46] Raman has been used to determine the structural characteristics of megacryometeors, including the altitude and temperature of formation.[75] Raman spectroscopy has also been used to study the atmospheric gasses that were contained in naturally occurring ice clathrates.[21] As mentioned above, standoff Raman systems have been used to measure ice from a distance of up to 120 meters.[22,76]

Biological Analytes. Biological analytes, or biomarkers, are vital to the discovery of life on other planets. The environments of target planets lead to the belief that extremophiles are likely biomarkers for discovery.[77] These include cyanobacteria and their pigments

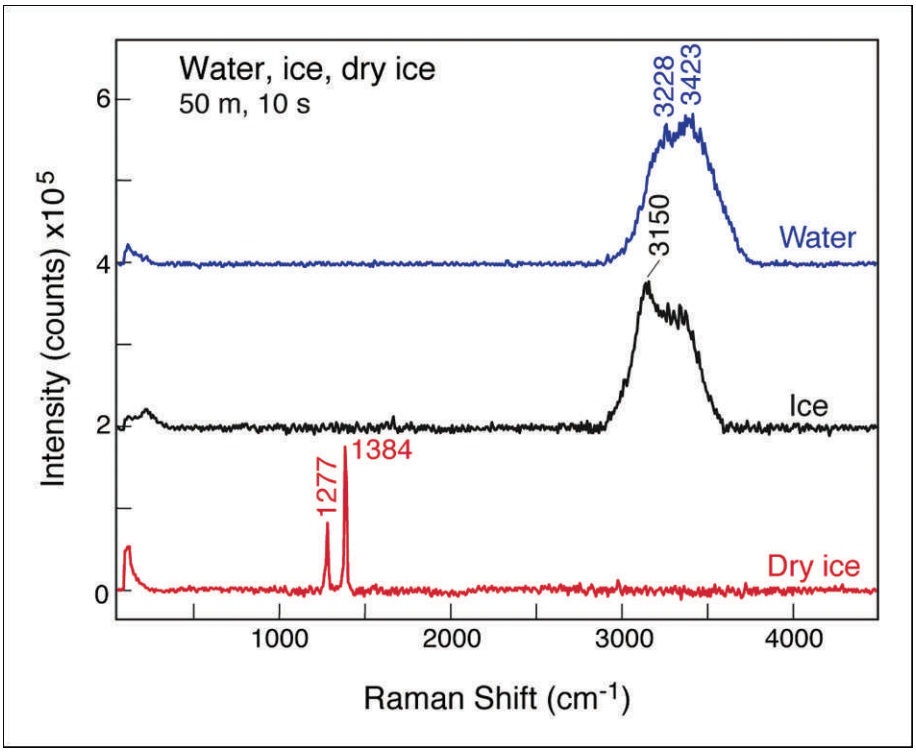

FIG. 8. Remote Raman spectra of water, ice, and dry ice (Reproduced with permission from Ref. 74).

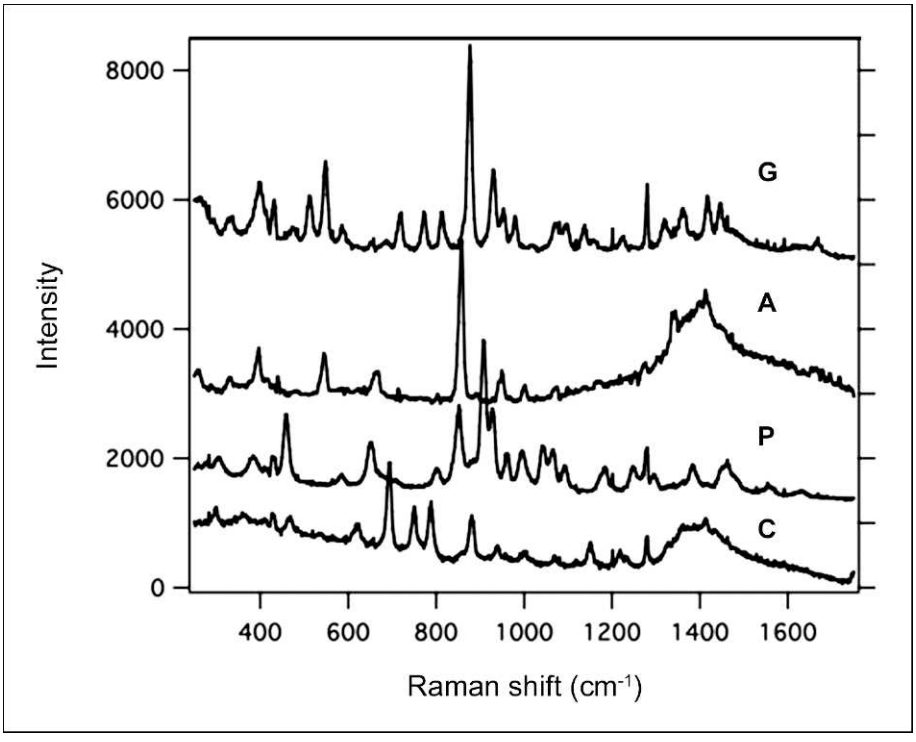

FIG. 9. Raman spectra of amino acids glutamic acid (G), alanine (A), proline (P), and cystiene (C).

in addition to other important pigments such as chlorophyll. Carotenoids, such as beta-carotene, and chlorophyll are some examples of important pigments. Amino acids are another important biomarker, and micro-Raman has been used to detect low amounts of amino acids by evaporating aqueous droplets containing femtomoles of proteins and measuring Raman spectra of the dry material.[68] Villar states that to detect biomarkers, a Raman system would need 16 cm^{-1} resolution in the spectral range from 500 to 1700 cm^{-1} for unambiguous identification.[78]

Amino acids have been studied extensively using Raman and Fig. 9 shows the Raman spectra of the amino acids glutamic acid, alanine, proline, and cystiene measured in our laboratory. Studies have shown Raman spectroscopy can be used to detect amino acids near femtomole levels and each amino acid can be distinguished looking at a range from 500 to 1700 cm^{-1} and that UV excitation is the best approach to their detection.[68] The strongest scattering amino acids are phenylalanine, tyrosine, tryptophan, cysteine and methionine.[68] Raman has also been used to distinguish amino acids based on their stereochemistry.[79] Culka made measurements of amino acids outside during the day, but covered the samples with a dark cloth.[80]

Pigments are also expected to be important biomarkers. Scytonemin is a UV pigment produced by cyanobacteria under stressed, or extreme, conditions. It is expected to be found in areas where extremophilic cyanobacteria are found, specifically indicating past life on Mars.[81] Scytonemin was discovered in the Rio Tinto area in Spain.[49,73] Carotenoids, like beta-carotene, can indicate the presence of algae or bacteria, and Raman has been proven capable of distinguishing between different types of carotenoids.[82] Sharma showed a time-resolved standoff system was capable of making Raman measurements of a tomato and a poinsettia leaf, thereby showing the capability of Raman to measure carotenoids in different matrices, including within a tomato (Fig. 10).[9] Diagenetically-reduced carotenoids are formed when biological material is fossilized, creating a possible

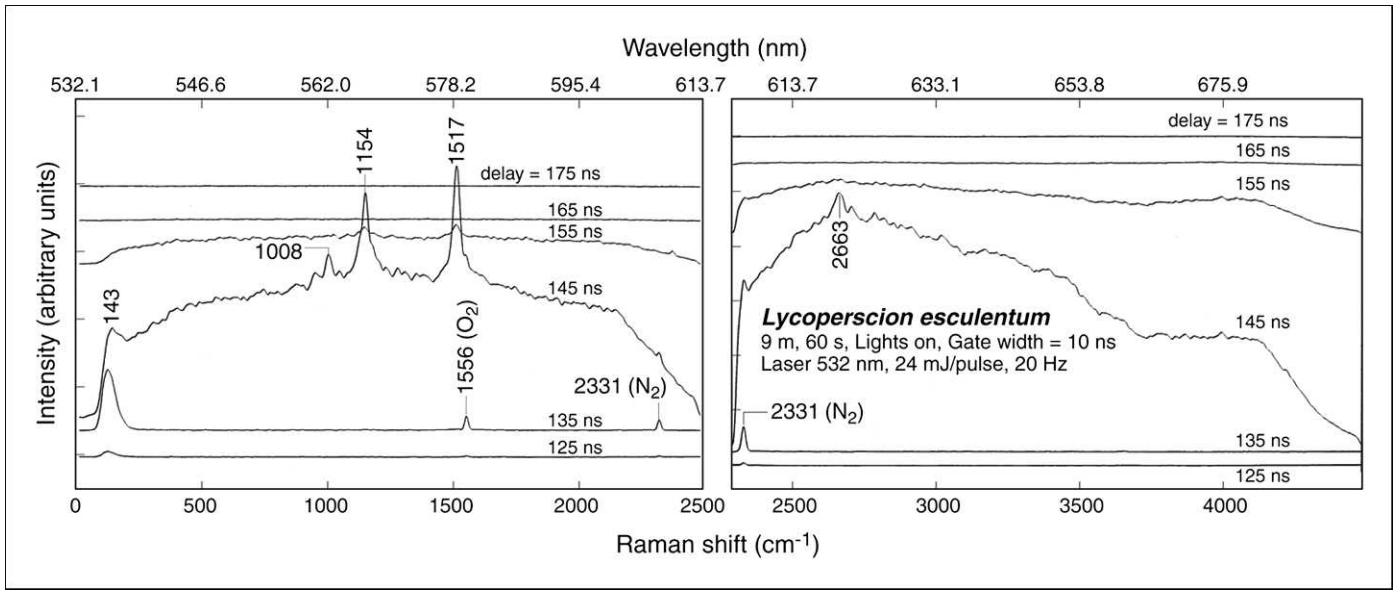

FIG. 10. Time-resolved Raman and fluorescence spectra of a tomato. The Raman bands at 1008 cm^{-1}, 1154 cm^{-1}, and 1517 cm^{-1} correspond to resonance Raman bands of β-carotene (Reproduced with permission from Ref. 9).

indicator of past life.[82] In addition, chlorophyll in leaves has been analyzed using standoff, time-resolved Raman systems.[83]

RAMAN COMBINED STANDOFF SYSTEMS

While Raman spectroscopy alone will be useful for planetary measurements, a Raman system combined with a second technique could prove to be invaluable for all future planetary missions, allowing a more complete determination of samples. Sharma stated that future trends in standoff planetary Raman will focus on combined systems.[9] He states that Raman combined with both LIBS and LIF has the capability of making remote measurements that contain mineralogical, biological, and elemental information, but may also include mass spectrometry. The following sections will describe combined Raman systems and discuss previous results for each combined technique.

Raman/Laser-Induced Breakdown Spectroscopy. A combined Raman/LIBS system would be a valuable tool for mineral analysis. LIBS utilizes high-powered laser pulses focused onto the sample to generate plasmas. The plasma is a result of the vaporization and subsequent atomization of the sample and within the plasma is the elemental information for the vaporized portion of the sample.[84] Raman spectrometry would be used to provide molecular information and detect organic molecules, while LIBS can determine elemental composition, including minor components in the sample.[84] The first standoff Raman/LIBS system was reported by Sharma et al. for planetary measurements.[7] The combined system was capable of 10-m standoff distances, where various silicates and carbonates were studied. The results showed that combining the cation data from LIBS with Raman anion data would allow remote identification and characterization of samples on planetary surfaces. Wiens et al. also developed a combined system for geological analysis and stated that a difficulty for combining the two techniques while sharing components is how to cover the larger spectral range for LIBS while maintaining the sensitivity for Raman.[84] Combined system standoff measurements have also been made under Martian conditions.[42,45] Sharma et al. stated that dust covering planetary samples could be removed using LIBS.[45] Misra et al. used a combined system to make measurements of water and ice samples through the walls of storage bottles.[76] As mentioned above, the upcoming Mars Science Lab mission will feature a LIBS system capable of standoff measurements up to 7 m, and the previously discussed ExoMars mission will incorporate a Raman/LIBS remote system, but not for standoff measurements.

Raman/Laser-Induced Fluorescence. Laser-induced fluorescence is also complementary to Raman spectroscopy. LIF is based on a molecule's absorption of energy and subsequent emission. LIF is much stronger and has a longer lifetime than Raman scattering, which is why fluorescence from impurities or a sample matrix can be a problem for Raman measurements. For Raman measurements, luminescence is typically avoided using UV or IR excitation or using pulsed lasers and gated detectors for time-resolved measurements. Time-resolved measurements allow for the separation of Raman and long-lived fluorescence, allowing each to be measured simultaneously with the same excitation source. LIF is useful for measuring trace amounts of inorganic materials and minerals, with detection limits near the parts per billion level, and is the most sensitive method for detection of organics and biomarkers.[9] Time-resolved LIF measurements can also differentiate between short-lived fluorescence from biological and organic materials and longer lived luminescence

from inorganic materials.[35] Sharma et al. developed the first Raman/LIF standoff system, which was capable of standoff measurements up to 100 meters.[3] The LIF portion of the system was capable of measurements up to 5 km, since fluorescence intensity is orders of magnitude higher than Raman scattering intensity. Bozlee et al. developed a combined system that measured LIF of minerals using excitation wavelengths in the UV and near-UV and used a gated 532 nm Raman system to measure various fluorescent samples.[35] Sharma reported that a Raman/LIF system operating at 532 nm would be ideal for detecting phytopigment biomarkers.[9]

OPTIMAL EXCITATION WAVELENGTH

An important consideration in standoff Raman is the choice of laser wavelength. In general short wavelengths are preferred over longer wavelengths because of the well known ν^4 dependence of Raman scattering and because of the possibility of resonance enhancement for highly absorbing molecules. However, there is much more that needs to be considered before deciding the best laser wavelength. Figure 11, line B, shows a plot of relative Raman scattering power versus wavelength, assuming a Raman cross-section of 10^{-28} cm^{-2} molecule^{-1} sr^{-1} at 450 nm with the cross-section scaling as λ^{-4} at other wavelengths. This is the expected wavelength behavior for normal Raman scattering power for a perfectly transparent sample with no resonance enhancement. However, using a photon detector a smaller power dependence may be observed,[85] so Fig. 11, line C, shows a λ^{-3} dependence.

A more important consideration in choosing the best laser wavelength is sample absorption. Even a small molar absorptivity can greatly affect the Raman signal as a result of decreased effective sample thickness. This is shown in lines D and E in Fig. 11, which shows the relative Raman signal for a sample with $\varepsilon = 100$ M^{-1}cm^{-1}, $\lambda_{max} = 450$ nm and a band width of 20 nm (see line A) for two different sample concentrations and thicknesses. For Fig. 11, line D, the sample is 0.1 cm thick and the concentration is 0.1 M. Even for this relatively non-absorbing sample, the Raman signal drops by 30–40% across the absorption region. This effect is much more severe for highly absorbing particles as is shown by line E in Fig. 11. In this case the sample thickness was chosen to be only 10 μm, but the sample concentration was chosen to be 10 M with a molar absorptivity of 1000 M^{-1}cm^{-1}, indicative of small, pure particle samples of an organic material. The attenuation of the Raman signal is severe even though the sample path length is microscopic, and the signal drops over a very wide range of wavelengths.

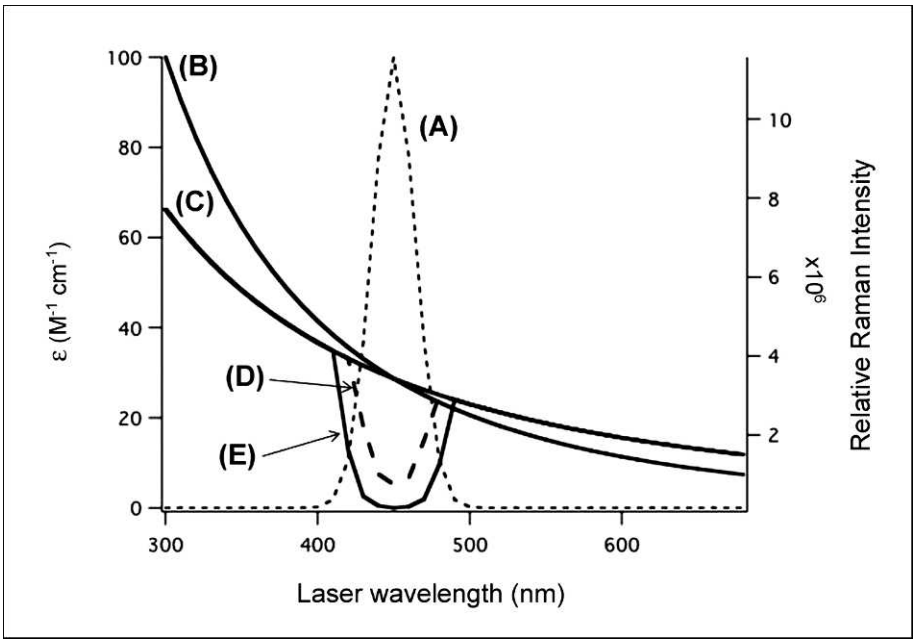

FIG. 11. (A) Absorption spectrum of the absorbing sample with $\varepsilon = 100$ and $\lambda_{max} = 450$ nm. Relative Raman signal level as a function of wavelength showing (B) λ^{-4} dependence for power measurements, and (C) λ^{-3} dependence for (D) a 0.1 M absorbing sample with $\varepsilon = 100$, 0.1 cm path length, and for (E) a 10 μm thick, 10^{-3} M sample with $\varepsilon = 1000$.

Resonance enhancement can provide a several thousand-fold increase in the Raman cross-section per molecule for samples that are highly absorbing. However, as shown in Fig. 12, this does not necessarily translate into an increase of 1000 or more in the measured signal. Figure 12 shows a series of plots of relative Raman signal versus wavelength for a case where the sample absorbs moderately strongly at 450 nm ($\varepsilon = 1000$ M^{-1}cm^{-1}), for a 0.1 cm sample path length, and using a Raman enhancement value at 450 nm of 1000 but for sample concentrations of (A) 1 mM, (B) 10 mM, (C) 100 mM, and (D) 1 M. The signal level is strongest in all cases where the molecule absorbs most strongly. However, the increase in Raman signal at around 450 nm, compared to the normal Raman on either side of the absorbing region, varies with concentration, with the largest increase of 667 being observed for the lowest concentration (1 mM) sample, dropping to less than 4 at the highest concentration of 1 M. In the case of higher concentrations of highly absorbing samples, the optimal wavelength is actually on the extreme high energy side of the absorption band, well removed from the λ_{max}. For low-concentration samples the optimal wavelength corresponds to the λ_{max}. However, the exact point where this behavior changes also depends on the Raman enhancement factor, sample or solute molar absorptivity, sample thickness, and sample concentration.

FUTURE STUDIES AND FEASIBILITY OF ORBITAL RAMAN MEASUREMENTS

There are more opportunities to place a Raman instrument in orbit around a planet or moon than to land. This brings up the question whether it is feasible to

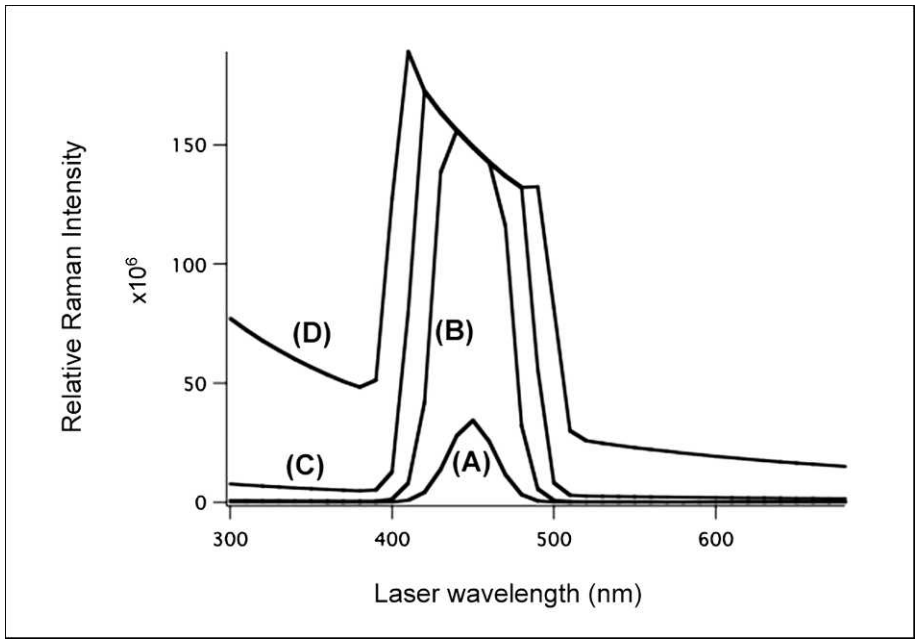

FIG. 12. Relative resonance Raman signal level as a function of wavelength for an absorbing sample ($\varepsilon = 1000$ and $\lambda_{max} = 450$ nm, with maximum resonance enhancement value of 1000 at λ_{max}) of different sample concentrations (A) 1 mM, (B) 10 mM, (C) 100 mM, and (D) 1 M.

acquire Raman spectra of surface features from an orbiting system. Obviously the answer should be "yes," given enough laser power and a large enough collection mirror. But is it realistic on a real mission? The answer is also "yes," as shown below.

In 2004 NASA made plans for an ambitious mission to explore the icy moons of Jupiter, concentrating on Europa. The proposed spacecraft called JIMO (Jupiter Moons Orbiter) was to be large enough to carry a 1–2 meter diameter collection mirror and would have enough power to operate a large ($\sim$1 J) pulsed laser. Initial planning was for an orbit as low as 10 km, but new plans increase this to 50 km or higher.

The Raman signal level can be calculated for an orbiting instrument using Eq. 1. Here the detected signal S (photoelectrons per pulse) is related to the laser power, P (photons pulse^{-1} cm^{-2}), Raman cross-section β (cm^2 molecule^{-1} sr^{-1}) for the molecule of interest, number density of molecules D (molecules cm^{-3}), sample path length K (cm), sample area viewed A (cm^2), collection solid angle Ω (sr), transmission of collection and measurement system T (unitless), and the quantum efficiency of the detector Q (e$^-$ per photon).

$$S = (P\beta DK)(A\Omega TQ) \qquad (1)$$

In this equation the terms in the first set of parentheses include sample and laser variables while the terms in the second set include collection and detector variables.

For an orbiter, the biggest unknowns in this equation are the sample concentration and path length (penetration depth). Sample concentrations are unknown but they may vary from 10 M to 55 M in the case of pure hydrocarbons on Titan or pure ice or water on Europa or Enceladus, to a few percent in the case of dark material on Europa's surface. The sample path length for a laser impinging on the surface may also vary widely from meters in the case of clear ice or water to millimeters or less in the case of highly absorbing, relatively pure materials adsorbed onto surface ice. The quantum efficiency and the other instrumental variables can be estimated with reasonable accuracy.

For the sake of this discussion we will use water and cyclohexane (C_6H_{12}), both of which have well-known Raman scattering cross-sections at 266 nm (3 and 25×10^{-27} cm^2 molecule^{-1} sr^{-1}, respectively) and at 532 nm. These two wavelengths are also selected because they are the second and third harmonics of the Nd:YAG laser, a system that is likely to be used on an orbiter. Pyrene is also used, with a well-known resonance Raman cross-section at 240 nm of 6.0×10^{-23} cm^2 molecule^{-1} sr^{-1}. We will assume a path length of 1 cm and, in the case of C_6H_{12} and pyrene, concentrations of 0.1 M and 1 mM, respectively. The high C_6H_{12} concentration is in line with early estimates of organic material concentrations of up to 8% on Europa's surface. In the case of water or ice we will assume the pure substance, $\sim$1 g/cm^3 concentration. The Raman signal is independent of laser spot size; however, the laser spot size on the surface is important to determine the spatial resolution of the measurements.

Table I shows calculated Raman signal levels for water, C_6H_{12}, and pyrene using 1 J/pulse 532 nm and 500 mJ/pulse 266 nm lasers, at 10 and 100 km orbital distances using a collection mirror 1 m in diameter, which corresponds to a 10^{-8} sr collection solid angle at 10 km. The laser power at 266 nm, 500 mJ, is close to the limit that is available from commercially available laboratory lasers. However, rapid advances are being made in space-qualified laser technology and it is feasible to couple many lower-power lasers to achieve the needed power. In all cases, with the possible exception of C_6H_{12} at 100 km using a single laser pulse, the signal levels are large enough to be measured against any reasonable background signal. For these calculations, a 1 cm path length seems modest and considering that the matrix in many cases will be ice, the path length might be much larger with correspondingly higher Raman signal levels. Also, using longer integration times, measuring at decreased spectral resolution, or measuring several wavelengths simultaneously (using imaging filters such as liquid crystal tunable filters), or using a slitless spectrometer, such as one that is based on an interferometer, might be

TABLE I. Calculated Raman signal levels (photoelectrons). Parameters used: 266 and 240 nm: $Q = .3$, $T = 0.8$, 532 nm: $Q = T = 0.8$.

Compound	10 km (1 J/pulse, 532 nm)	100 km (1 J/pulse, 532 nm)	10 km (0.5 J/pulse, 266 nm)[a]	100 km (0.5 J/pulse, 266 nm)[a]
H_2O (100 pulses)			1.6×10^7	1.6×10^5
C_6H_{12} (100 pulses)	1.6×10^5	6.6×10^3	2.4×10^5	2.4×10^3
Pyrene (100 pulses)			$5.8 \times 10^{6,a}$	$5.8 \times 10^{4,a}$
H_2O (one pulse)			1.6×10^5	1.6×10^3
C_6H_{12} (one pulse)	1.6×10^3	6.6×10^1	2.4×10^3	2.4×10^1
Pyrene (one pulse)			$5.8 \times 10^{4,a}$	$5.8 \times 10^{2,a}$

[a] Pyrene calculations were done assuming a resonance Raman cross-section of 6.0×10^{-23} cm^2 molecule^{-1} sr^{-1} at 240 nm, concentration of 1 mM, and a 1 cm path length.

used to further increase signal levels. These results certainly show enough promise to justify further investigation of the feasibility of measuring Raman spectra from an orbiting spacecraft in a low altitude orbit. The signal levels might at first seem high, but the concentrations and cross-sections are realistic and the instrument is one that was seriously considered for the JIMO mission.

Background signals always limit the signal-to-noise ratio of Raman measurements and thus the detection limit. It is impossible to predict the background levels but they might be low considering the use of a fast-pulsed laser to discriminate against ambient light and long-lived background luminescence, along with the choice of two different wavelengths to help minimize background fluorescence.

The spatial resolution that can be achieved during a Raman measurement depends on the measurement scenario. An orbiter around Europa would have an orbital velocity of around 1.3 km/s. Assuming a 1 meter focused laser spot on the surface (the diffraction limit at 100 km is only 0.13 meters) and a 7 ns pulsed laser, the laser spot will move only about 10 μm for each pulse. Thus, the spatial resolution for single-pulse measurements can be as small as the laser spot. For a moon like Europa, there is no real atmosphere to distort the laser beam, so focusing the laser to a spot much smaller than 1 m should be feasible. The spatial resolution increases if many pulses are averaged. For an integration time of 1 s (10 pulses at 10 Hz, 100 pulses for 100 Hz laser), the total surface path of the laser would be 1.3 km, measured as 1 meter spots, each separated by 130 meters in the case of a 100 Hz laser. Fast slewing might be used to improve the spatial resolution and also allow longer integration times. By slewing, any given point on the surface can be viewed for a few minutes but with an ever increasing range.

A more interesting and useful method to increase the spatial resolution while averaging a large number of laser pulses might involve using a post-measurement algorithm, where the Raman signals for all laser pulses are saved for a large number of orbits. High-resolution images using a conventional camera would presumably allow the surface location for every laser pulse to be accurately determined. Post-processing of the accumulated Raman signals would involve adding Raman signals from areas that were found to be visually or otherwise optically similar. In this way Raman surface maps with high signal-to-noise ratio could be developed, with spatial resolution limited only by the size of the laser spot and by the ability to locate the laser spot on the surface. For example, thousands of different laser pulses might be integrated from all over the surface, to produce a single high signal-to-noise ratio Raman spectrum, for regions on the surface with a certain reflectivity. The spatial resolution in this case, assuming a 1 m^2 laser spot on the surface, would be 1000 m^2.

CONCLUSIONS

Standoff Raman systems have been described that are suitable for measuring inorganic and organic compounds of the type that are of interest to planetary scientists and at concentration levels that are relevant to planetary applications and astrospectroscopy. Such measurements have also been made using a variety of spectrometer designs over large distances, from tens to hundreds of meters. There are also Raman spectrometers that have been designed specifically to land on Mars for proximal and standoff measurements. Calculations show that it is theoretically possible to measure Raman spectra from an orbiting spacecraft, using a moderately large mirror and large pulsed laser.

ACKNOWLEDGMENTS

The authors at USC would like to thank NSF for funding for some of the work presented under CHE 0526821, and additional thanks goes to DOE/Lawrence Livermore National Laboratory for equipment and supplies. The work at the University of Hawaii was supported in part by NASA under a MIDDP grant NNX08AR10G.

1. A. Wang, B. L. Jolliff, and L. A. Haskin, J. Geophys. Res.-Planets, **100,** 21189 (1995).
2. L. A. Haskin, A. Wang, K. M. Rockow, B. L. Jolliff, R. L. Korotev, and K. M. Viskupic, J. Geophys. Res. **102,** 19293 (1997).
3. S. K. Sharma, S. Ismail, S. M. Angel, P. G. Lucy, C. P. McKay, A. K. Misra, P. J. Mouginis-Mark, H. Newsom, U. N. Singh, and G. J. Taylor, Proc. SPIE-Int. Soc. Opt. Eng. **5660,** 128 (2004).
4. S. M. Clegg, J. E. Barefield, R. C. Wiens, C. R. Quick, S. K. Sharma, A. K. Misra, M. D. Dyar, M. C. McCanta, and L. Elkins-Tanton, Workshop on Venus Geochemistry: Progress, Prospects, and New Missions February 26–27, 2009, (Gilruth Center, NASA Johnson Space Center, Houston, TX, 2009).
5. S. Sharma, A. K. Misra, and T. Acosta, Phil. Trans. R. Soc. A **368,** 3167 (2010).
6. S. K. Sharma, S. M. Angel, M. Ghosh, H. W. Hubble, and P. G. Lucey, Appl. Spectrosc. **56,** 699 (2002).
7. S. K. Sharma, P. G. Lucey, M. Ghosh, H. W. Hubble, and K. A. Horton, Spectrochim. Acta, Part A **59,** 2391 (2003).
8. A. K. Misra, S. K. Sharma, C. H. Chio, P. G. Lucey, and B. Lienert, Spectrochim. Acta, Part A **61,** 2281 (2005).
9. S. K. Sharma, Spectrochim. Acta, Part A **68,** 1008 (2007).
10. C. V. Raman, Nature **121,** 69 (1928).
11. S. K. Sharma, Vib. Spectra Struct. **17B,** 513 (1989).
12. A. Wang, J. Han, L. Guo, J. Yu, and P. Zeng, Appl. Spectrosc. **48,** 959 (1994).
13. I. A. Degen and G. A. Newman, Spectrochim. Acta, Part A **49,** 859 (1993).
14. P. F. McMillan and A. M. Hofmeister, Rev. Miner. **18,** 103 (1988).
15. K. Nakamoto, *Infrared and Raman Spectra of Inorganic and Coordination Compounds* (John Wiley and Sons, New York. 1997), 5th ed.
16. R. W. Gauldie, S. K. Sharma, and E. Volk, Comp. Biochem. Physiol. **119A,** 753 (1997).
17. S. K. Sharma and J. P. Urmos, *Microbeam*

Analysis (San Francisco Press Inc, San Francisco, CA, 1987), pp. 133–136.
18. M. J. Taylor and E. Whalley, J. Chem. Phys. **40,** 1660 (1964).
19. H. C. Cynn, S. Boone, A. Koumvakalis, M. Nicol, and D. J. Stevenson, Proc. Lunar Planet. Sci. Conf. **19,** 433 (1989).
20. J. P. Devlin, J. Chem. Phys. **90,** 1322 (1989).
21. F. Pauer and J. Kipfstuhl, Geophys. Res. Lett. **22,** 969 (1995).
22. S. K. Sharma, A. K. Misra, and B. Sharma, Spectrochim. Acta, Part A **61,** 2404 (2005).
23. J. Cooney in *Proceedings of the Symposium on Electromagnetic Sensing of the Earth from Satellites*, R. Zirkind, Ed. (Polytechnic P., Brooklyn, NY, 1965), p. 1.
24. T. Hirschfeld, S. Klainer, and R. Burton, in *Proceedings of the Electrooptical Systems Design Symposium*, K. A. Kopetzsky, Ed. (Industrial and Scientific Conference Management, Chicago. IL, 1970), p. 418.
25. T. Hirschfeld, E. R. Schildkraut, H. Tannenbaum, and D. Tannenbaum, Appl. Phys. Lett. **22,** 38 (1973).
26. T. Hirschfeld, Appl. Opt. **13,** 1435 (1974).
27. S. M. Angel and T. J. Kulp, Appl. Spectrosc. **46,** 1085 (1992).
28. J. C. Carter, S. M. Angel, M. Lawrence-Snyder, J. Scaffidi, R. E. Whipple, and J. G. Reynolds, Appl. Spectrosc. **59,** 769 (2005).
29. S. K. Sharma, A. K. Misra, P. G. Lucey, S. M. Angel, and C. P. McKay, Appl. Spectrosc. **60,** 871 (2006).
30. T. Chen, J. M. J. Madey, S. K. Sharma, and B. Lienert, Appl. Spectrosc. **61,** 624 (2007).
31. M. Wu, M. Ray, K. H. Fung, M. W. Ruckman, D. Harder, and A. J. Sedlacek III, Appl. Spectrosc. **54,** 800 (2000).
32. J. C. Carter, J. Scaffidi, S. Burnett, B. Vasser, S. K. Sharma, and S. M. Angel, Spectrochim. Acta, Part A **61,** 2288 (2005).
33. V. Klein, J. Popp, N. Tarcea, M. Schmitt, W. Kiefer, S. Hofer, T. Stuffler, M. Hilchenbach, D. Doyle, and M. Dieckmann, J. Raman Spectrosc. **35,** 433 (2004).
34. A. J. Hobro and B. Lendl, TrAC, Trends Anal. Chem. **28,** 1235 (2009).
35. B. J. Bozlee, A.K. Misra, and S. Sharma, Spectrochim. Acta, Part A **61,** 2342 (2005).
36. A. K. Misra, S. K. Sharma, and P. G. Lucey, Appl. Spectrosc. **60,** 223 (2006).
37. M. Gaft and L. Nagli, Opt. Mater. **30,** 1739 (2008).
38. I. Johansson, S. Wallin, M. Nordberg, and H. Ostmark, Propellants Explos. Protech. **34,** 297 (2009).
39. J. N. Porter, C. E. Helsley, S. K. Sharma, A. K. Misra, D. E. Bates, and B. R. Lienart, J. Raman Spectrosc., doi: 10.1002/jrs.2998 (2011).
40. J. D. Stopar, P. G. Lucey, S. K. Sharma, A. K. Misra, and H. W. Hubble, Spectrochim. Acta, Part A **61,** 2315 (2005).
41. S. K. Sharma, A. K. Misra, S. M. Clegg, J. E. Barefield, R. C. Wiens, T. E. Acosta, and D. E. Bates, Spectrochim. Acta, Part A **80,** 75 (2011).
42. C. B. Dreyer and G. S. Mungas, Lunar and Planetary Science XXXVIII, 2307 (2007).
43. A. Ellery and D. W.-Williams, Astrobiology **3,** 565 (2003).
44. A. Wang· J. J. Freeman, B. L. Jolliff, and I-M. Chou, Geochim. Cosmochim. Acta. **70,** 6118 (2006).
45. S. K. Sharma, A. K. Misra, P. G. Lucey, R. C. Wiens, and S. M. Clegg, Spectrochim. Acta, Part A **68,** 1036 (2007).
46. F. Rull, A. Vegas, A. Sansano, and P. Sobron, Spectrochim. Acta, Part A **80,** 148 (2011).
47. H. G. M. Edwards and J. Jehlicka, Phil. Trans. R. Soc. A **368,** 3099 (2010).
48. S. E. Jorge-Villar and H. G. M. Edwards, Phil. Trans. R. Soc. A **368,** 3127 (2010).
49. H. G. M. Edwards, P. Vandenabeele, S. E. Jorge-Villar, E. A. Carter, F. Rull Perez, and M. D. Hargreaves, Spectrochim. Acta, Part A **68,** 1133 (2007).
50. A. Wang, B. L. Jolliff, and L.A. Haskin, J. Geophys. Res. **104,** 8509 (1999).
51. T. F. Cooney, E. R. D. Scott, A. N. Krot, S. K. Sharma, and A. Yamaguchi, Am. Mineral. **84,** 1569 (1999).
52. A. Wang, K. Kuebler, B. Jolliff, and A. L. Haskin, J. Raman Spectrosc. **35,** 504 (2004).
53. P. Mahaffy, C. R. Webster, M. Cabane, and P. G. Conrad, Space Science Reviews, paper in press (2012).
54. R. C. Wiens, S. Maurice, B. Barraclough, and M. Saccoccio, Space Science Reviews, paper in press (2012).
55. A. Wang, L. A. Haskin, A. L. Lane, T. J. Wdowiak, S. W. Squyres, R. J. Wilson, L. E. Hovland, K. S. Manatt, N. Raouf, and C. D. Smith, J. Geophys. Res. **108,** 5005 (2003).
56. A. Wang, L. A. Haskin, and E. Cortez, Appl. Spectrosc. **52,** 477 (1998).
57. V. I. Moroz, Adv. Space Res. **29,** 215 (2002).
58. Z. C. Ling, A. Wang, and B. L. Jolliff, Icarus, **211,** 101 (2011).
59. M. H. Carr, M. J. S. Belton, C. R. Chapman, M. E. Davies, and P. Geissler, Nature, **391,** 363 (1998).
60. R. T. Pappalardo, M. J. S. Belton, H. H. Breneman, M. H. Carr, and C. R. Chapman, J. Geophys. Res. **104,** 24015 (1999).
61. M. G. Kivelson, K. K. Khurana, C. T. Russell, M. Volwerk, R. J. Walker, and C. Zimmer, Science **289,** 1340 (2000).
62. C. F. Chyba and C. B. Phillips, Proc. Natl Acad. Sci. USA **98,** 801 (2001).
63. C. C. Porco, P. Helfenstein, P. C. Thomas, A. P. Ingersoll, and J. Wisdom, Science **311,** 1393 (2006).
64. J. H. Waite Jr., M. R. Combi, W. H. Ip, T. E. Cravens, and R. L. McNutt, Jr., Science **311,** 1419 (2006).
65. J. H. Waite, Jr., W. S. Lewis, B. A. Magee, J. I. Lunine, and W. B. McKinnon, Nature, **460,** 487 (2009).
66. C. P. McKay, C. C. Porco, T. Altheide, W. L. Davis, and T. A. Kral, Astrobiology, **8,** 909 (2008).
67. J. L. Bada, P. Ehrenfreund, F. Grunthaner, D. Blaney, and M. Coleman, Space Sci. Rev. **135,** 269 (2008).
68. A. L. Jenkins, R. A. Larsen, and T.B. Williams, Spectrochim. Acta, Part A **61,** 1585 (2005).
69. Z. C. Ling and A. Wang, Icarus **209,** 422 (2010).
70. W. G. Kong, A. Wang, J. J. Freema, and P. Sobron, J. Raman Spectrosc. **42,** 1120 (2011).
71. J. J. Freeman, A. Wang, K. E. Kuebler, B. L. Jolliff, and L. A. Haskin, Can. Miner. **46,** 1477 (2008).
72. K. E. Kuebler, B. L. Jolliff, A. Wang, and L. A. Haskin, Geochim. Cosmochim. Acta **70,** 6118 (2006).
73. P. Sobron, A. Sanz, T. Acosta, and F. Rull, Spectrochim. Acta, Part A **71,** 1678 (2009).
74. S. K. Sharma, A. K. Misra, T. E. Acosta, P. G. Lucey, and M. N. Abedin, Proc. SPIE-Int. Soc. Opt. Eng. **7691,** 76910F/1 (2010).
75. F. Rull and J. Martinez-Frias, Phil. Trans. R. Soc. A. **368,** 3145 (2010).
76. A. K. Misra, S. K. Sharma, T. E. Acosta, and D. E. Bates, Proc. SPIE-Int. Soc. Opt. Eng. **8032,** 24 (2011).
77. S. E. Villar and H. G. M. Edwards, Anal. Bioanal. Chem. **384,** 100 (2006).
78. S. E. Jorge-Villar and H. G. M. Edwards, Int. J. Astrobiol. **3,** 165 (2004).
79. L. A. Nafie, G. S. Yu, and T. B. Freedman, Vib. Spectrosc. **8,** 231 (1995).
80. A. Culka, J. Jehlicka, and H. G. M. Edwards, Spectrochim. Acta, Part A **77,** 978 (2010).
81. T. Varnali and H. G. M. Edwards, Phil. Trans. R. Soc. A **368,** 3193 (2010).
82. C. P. Marshall and A. O. Marshall, Phil. Trans. R. Soc. A **368,** 3137 (2010).
83. C. S. Garcia, M. N. Abedin, S. Ismail, S. K. Sharma, A. K. Misra, T. Nyugen, and H. Elsayed-Ali, Proc. SPIE-Int. Soc. Opt. Eng. **7312,** 731210 (2009).
84. R. C. Wiens, S. K. Sharma, J. Thompson, A. Misra, and P. G. Lucey, Spectrochim. Acta, Part A **61,** 2324 (2005).
85. T. Hirschfeld and B. Chase, Appl. Spectrosc. **40,** 133 (1986).